Mixed-Metal Cluster Chemistry. 39. Syntheses and X-ray Structures of $Mo_3Ir_3(\mu_4\text{-}\eta^2\text{-}CO)(\mu_3\text{-}CO)(CO)_{10}(\eta^5\text{-}C_5H_5)_3$ and $Mo_3RhIr_3(\mu\text{-}CO)_4(CO)_7(\eta^5\text{-}C_5H_5)_3(\eta^5\text{-}C_5Me_5)$**

Junhong Fu, Michael D. Randles, Graeme J. Moxey, Rob Stranger, Marie P. Cifuentes, and Mark G. Humphrey*

Research School of Chemistry, Australian National University, Canberra, ACT 2601 (Australia)

ABSTRACT

Thermolysis of tetrahedral $Mo_2Ir_2(\mu\text{-}CO)_3(CO)_7(\eta^5\text{-}C_5H_5)_2$ in refluxing toluene affords small amounts of $Mo_3Ir_3(\mu_4\text{-}\eta^2\text{-}CO)(\mu_3\text{-}CO)(CO)_{10}(\eta^5\text{-}C_5H_5)_3$ (**1**). Reaction of **1** with $Rh(CO)_2(\eta^5\text{-}C_5Me_5)$ in refluxing dichloromethane gives $Mo_3RhIr_3(\mu\text{-}CO)_4(CO)_7(\eta^5\text{-}C_5H_5)_3(\eta^5\text{-}C_5Me_5)$ (**2**) in moderate yield. X-ray diffraction studies show the metal cores adopt edge-bridged trigonal bipyramidal and bicapped trigonal bipyramidal structures, respectively. Cluster **2** is electron precise with 96 CVE, in contrast to the only precedent group 6-group 9 mixed-metal cluster with an identical core geometry, the 94 CVE $W_3Ir_4(\mu\text{-}H)(CO)_{12}(\eta^5\text{-}C_5H_5)_3$ (**3**). DFT studies have been employed to rationalize the contrasting behavior of **2** and **3**. Time-dependent DFT has been employed to assign the key transitions in the linear optical absorption spectrum of **2**.

Keywords: Molybdenum; Rhodium; Iridium; Carbonyl; Cluster

* Corresponding author.

E-mail address: Mark.Humphrey@anu.edu.au; ph: +61 2 6125 2927; fax: +61 2 6125 0750.

** Contribution to the Special Issue of the Journal of Organometallic Chemistry on "Frontiers in Organometallic Chemistry".

1. Introduction

Mixed-metal cluster chemistry has been of long-standing interest due to its relevance to catalysis and advanced materials.[1-3] The presence of differing transition metals may offer molecular approaches to the design of catalysts with high activity and selectivity, because the intrinsic polarity of heterometallic bonds may afford enhanced activation and direct the selectivity of substrate-cluster interactions.[4,5] Mixed-metal clusters can possess readily tailored physical properties (such as optical limiting) because of facile structural manipulation resulting from incorporation of differing metal atoms and the variation of the metal core skeletons,[6] so they continue to command attention.

Amongst the many possible clusters, those containing metal atoms from groups 6 and 9 have attracted considerable interest,[7] because clusters with these diverse metals can be stabilized by a common cyclopentadienyl/carbonyl ligand sheath. We have reported comprehensive studies of the syntheses and chemistry of low-nuclearity tetranuclear mixed molybdenum/tungsten-iridium carbonyl clusters,[8] and have recently extended these studies to pentanuclear examples,[9] although medium- and high-nuclearity heterometallic clusters remain comparatively underexploited.[10] We have continued to explore the syntheses of higher-nuclearity examples and herein report the syntheses of $Mo_3Ir_3(\mu_4\text{-}\eta^2\text{-}CO)(\mu_3\text{-}CO)(CO)_{10}(\eta^5\text{-}C_5H_5)_3$ (**1**) and $Mo_3RhIr_3(\mu\text{-}CO)_4(CO)_7(\eta^5\text{-}C_5H_5)_3(\eta^5\text{-}C_5Me_5)$ (**2**), their X-ray structural confirmation, and theoretical studies of **2** and the structurally related cluster $W_3Ir_4(\mu\text{-}H)(CO)_{12}(\eta^5\text{-}C_5H_5)_3$ (**3**) rationalizing their differing electron counts.

2. Results and discussion

*2.1. Synthesis of $Mo_3Ir_3(\mu_4\text{-}\eta^2\text{-}CO)(\mu_3\text{-}CO)(CO)_{10}(\eta^5\text{-}C_5H_5)_3$ (**1**) and $Mo_3RhIr_3(\mu\text{-}CO)_4(CO)_7(\eta^5\text{-}C_5H_5)_3(\eta^5\text{-}C_5Me_5)$ (**2**).*

Thermolysis of the tetrahedral cluster $Mo_2Ir_2(\mu\text{-}CO)_3(CO)_7(\eta^5\text{-}C_5H_5)_2$ in refluxing toluene for 30 min afforded a complex mixture of products that was separated by preparative thin-layer chromatography. The new hexanuclear cluster $Mo_3Ir_3(\mu_4\text{-}\eta^2\text{-}CO)(\mu_3\text{-}CO)(CO)_{10}(\eta^5\text{-}C_5H_5)_3$ (**1**, Scheme 1) was obtained as a brown solid in 16% yield and characterized by IR and ^{1}H NMR spectroscopy, ESI mass spectrometry, and satisfactory elemental analyses, and

definitively identified by a single-crystal X-ray diffraction study (see below). The solution IR spectrum of **1** contains ten *ν*(CO) bands, eight of which correspond to terminally-bound carbonyls (2067−1929 cm^{-1}) and two of which correspond to bridging carbonyl modes (1878 and 1698 cm^{-1}). The ^1H NMR spectrum contains three resonances assigned to the molybdenum-bound cyclopentadienyl groups at 5.72, 5.44 and 5.34 ppm, while the ESI mass spectrum shows a molecular ion peak with the correct characteristic isotope pattern at 1397 mass units. Treatment of **1** with an excess of $Rh(CO)_2(\eta^5\text{-}C_5Me_5)$ in refluxing CH_2Cl_2 for 24 h afforded a mixture containing unreacted starting cluster (43%) and the heptanuclear trimetallic cluster $Mo_3RhIr_3(\mu\text{-}CO)_4(CO)_7(\eta^5\text{-}C_5H_5)_3(\eta^5\text{-}C_5Me_5)$ (**2**, Scheme 1), isolated as a brown solid after TLC in 42% yield. Varying the reactions conditions for the syntheses of both **1** and **2** did not improve the yields. Cluster **2** shows five *ν*(CO) bands in the solution IR spectrum, three corresponding to terminal- (2023−1941 cm^{-1}) and two to bridging- carbonyl modes (1797 and 1711 cm^{-1}). The ^1H NMR spectrum of **2** contains three resonances assigned to the molybdenum-bound cyclopentadienyl groups at 5.33, 5.28 and 4.82 ppm, and a signal at 2.10 ppm attributed to the rhodium-bound pentamethylcyclopentadienyl group. The ESI mass spectrum shows the molecular ion with the correct isotope pattern at 1613 mass units. The identity of cluster **2** was conclusively established from a single-crystal X-ray diffraction study.

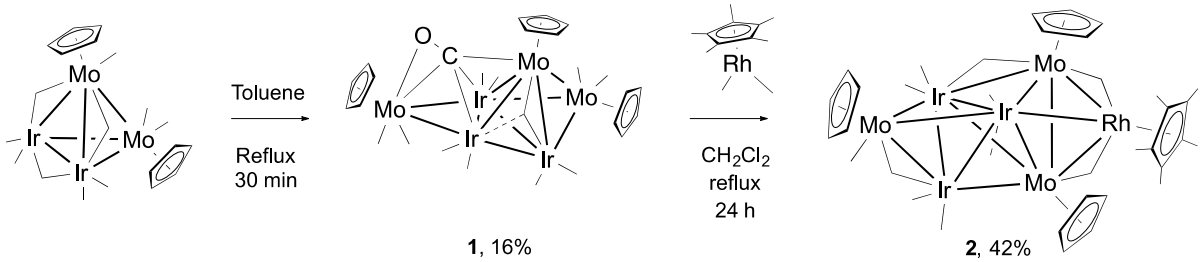

Scheme 1. Syntheses of $Mo_3Ir_3(\mu_4\text{-}\eta^2\text{-}CO)(\mu_3\text{-}CO)(CO)_{10}(\eta^5\text{-}C_5H_5)_3$ (**1**) and $Mo_3RhIr_3(\mu\text{-}CO)_4(CO)_7(\eta^5\text{-}C_5H_5)_3(\eta^5\text{-}C_5Me_5)$ (**2**).

*2.2. X-ray structural studies of **1** and **2***

ORTEP plots with the molecular structure, atomic labeling schemes and a selection of bond lengths and angles for clusters **1** and **2** are shown in Figures 1 and 2, respectively, while

Table S1 in the ESI contains relevant crystallographic acquisition data and refinement parameters. Cluster **1** possesses an edge-bridged trigonal bipyramidal metal core with two of the molybdenum atoms in apical and equatorial sites of the trigonal bipyramid and the third molybdenum bridging an Ir_{ap}–Ir_{eq} vector. Each of the molybdenum atoms is ligated by a η^5-cyclopentadienyl ligand, and twelve carbonyl groups (ten terminal, one semi-face-capping and one μ_4-η^2-bridging) complete the ligand set. The μ_3-CO (CO234) bridges a Mo–Ir bond and is significantly displaced towards a second iridium atom (with asymmetry parameters α = 0.09 (Ir3−Ir2), 0.16 (Ir3−Mo4) and 0.26 (Ir2−Mo4)).[11] The μ_4-η^2-CO ligand (CO126) sits in the butterfly cleft formed by Mo6 bridging Ir1-Ir2 and inclined towards the Ir1Ir2Mo4 face. The Ir−Ir [2.6730(7)−2.7856(7) Å], Ir−Mo [2.7648(13)−2.9004(11) Å], and Mo−Mo [2.9371(15) Å] bond distances lie within the range of literature precedents.[10,12]

The cluster possesses 3 × 6(Mo) + 3 × 9(Ir) + 10 × 2(CO_t) + 1 x 2(CO_b) + 1 x 4(μ_4-η^2-CO)

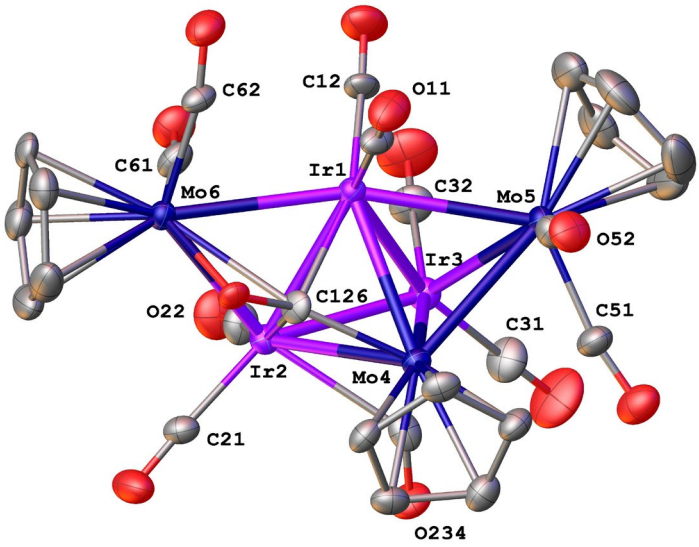

Figure 1. ORTEP plot and atom numbering scheme for $Mo_3Ir_3(\mu_4$-η^2-$CO)(\mu_3$-$CO)(CO)_{10}(\eta^5$-$C_5H_5)_3$ (**1**). Displacement ellipsoids are shown at the 40% probability level. Hydrogen atoms have been omitted for clarity. The thicker bonds depict the edge-bridged trigonal bipyramidal cluster core. Selected bond lengths (Å): Ir1−Ir2 2.7856(7), Ir1−Ir3 2.7654(6), Ir1−Mo4 2.8166(11), Ir1−Mo5 2.8783(12), Ir1−Mo6 2.9004(11), Ir2−Ir3 2.6730(7), Ir2−Mo4 2.8653(11), Ir2−Mo6 2.8220(11), Ir3−Mo4 2.8724(11), Ir3−Mo5 2.7648(13), Mo4−Mo5 2.9371(15), Ir1−C11 1.899(12), Ir1−C12 1.924(12), Ir1−C126 2.167(12), Ir2−C21 1.874(13), Ir2−C22 1.898(13), Ir2−C126 2.142(11), Ir2−C234 2.509(15), Ir3−C31 1.889(15), Ir3−C32 1.889(14), Ir3−C234 2.305(15), Mo4−C126 2.009(11), Mo4−C234 1.995(13), Mo5−C51 1.970(14), Mo5−C52 1.965(14), Mo6−C61 2.007(13), Mo6−C62 1.977(12), Mo6−C126 2.507(12), Mo6−O126 2.160(8).

+ 3 × 5(Cp) = 86 CVE, which is EAN-precise for a hexanuclear cluster with 11 M−M bonds, and PSEPT-precise for condensed polyhedra consisting of a trigonal bipyramidal core fused with a triangle by means of a common edge (72 + 48 - 34 = 86 electrons). The core atom disposition in **1** is not unusual, with precedents including the (methylcyclopentadienyl)tungsten-containing analogue $W_3Ir_3(\mu_4\text{-}\eta^2\text{-}CO)(\mu\text{-}CO)(CO)_{10}(\eta^5\text{-}C_5H_4Me)_3$[13] and the recently reported electron-precise cluster $Mo_3Ir_3(\mu_3\text{-}O)(\mu\text{-}CO)_3(CO)_8(\eta^5\text{-}C_5H_5)_3$.[10]

The metal core of cluster **2** adopts a bicapped trigonal-bipyramidal geometry, consisting of a central Mo_2Ir_3 trigonal bipyramid with the molybdenum atoms in apical and equatorial sites, a rhodium capping an $IrMo_2$ face, and the third molybdenum capping the unique Ir_3 face. The molybdenum atoms are each ligated by a η^5-cyclopentadienyl ligand, the rhodium is ligated by a η^5-pentamethylcyclopentadienyl ligand, and the coordination geometry is completed by seven terminal and four bridging carbonyl ligands, two bridging Rh–Mo and two bridging Ir–Mo bonds. The former μ-CO ligands (CO17, CO47) are displaced very slightly towards the molybdenum atoms of the Mo1-Rh7 and Mo4-Rh7 vectors, respectively, whereas the latter (CO34 and CO56) are formally semi-bridging, being displaced significantly towards the Mo atom (Curtis semi-bridging parameters 0.22 and 0.30, respectively).[11] All metal-metal bond distances lie within the range of literature precedents.[9,10] Cluster **2** contains 3 × 6(Mo) + 3 × 9(Ir) + 1 × 9(Rh) + 7 × 2(CO_t) + 4 x 2(CO_b) + 3 × 5(Cp) + 1 × 5(Cp*) = 96 CVE, which is the EAN-expected count for a heptanuclear cluster with 15 M-M bonds, and the PSEPT-predicted count for condensed polyhedra consisting of two trigonal bipyramids fused by means of a shared face (72 + 72 - 48 = 96 electrons).

The bicapped trigonal-bipyramidal core geometry of **2** is unusual for heptametallic clusters for which a capped octahedral geometry is most commonly seen. We have therefore examined extant examples of this geometry. There are three possible metal core arrangements for bicapped trigonal-bipyramidal clusters, classified as types A, B and C in Figure 3. Examples of type A are primarily group 8 metal/gold-containing clusters with 96 CVE, as predicted by the polyhedral skeletal electron pair theory (PSEPT) for bicapped trigonal-bipyramidal polyhedra.[14] One exception to this general composition is $Os_3Rh_4(\mu_3\text{-}\eta^6\text{-}C_6H_5CH_3)(CO)_{13}$ with a CVE count of 92, the formal electron deficiency of which was rationalized by analogy with homometallic rhodium clusters that have been shown to

sometimes conform to the 16-electron rule instead of the 18-electron rule.[15,16] No examples of Type B have been reported so far.

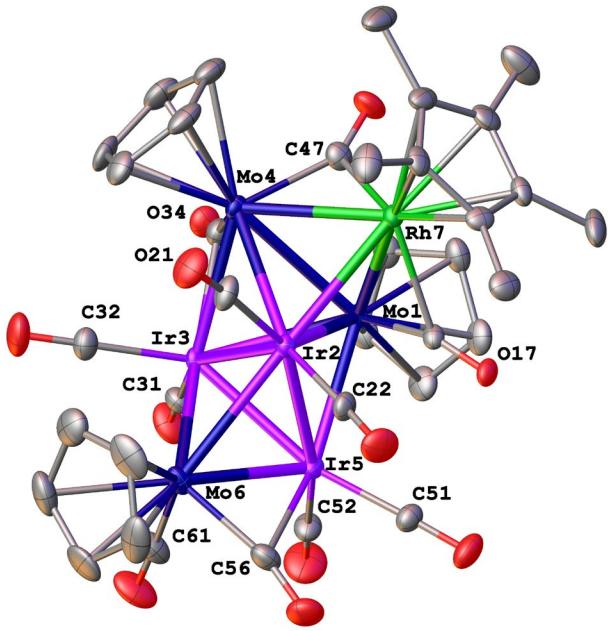

Figure 2. ORTEP plot and atom numbering scheme for $Mo_3RhIr_3(\mu\text{-}CO)_4(CO)_7(\eta^5\text{-}C_5H_5)_3(\eta^5\text{-}C_5Me_5)$ (**2**). Displacement ellipsoids are shown at the 40% probability level. Hydrogen atoms and the lattice methanol molecule have been omitted for clarity. The thicker bonds depict the bicapped trigonal bipyramidal cluster core. Selected bond lengths (Å): Ir2−Mo1 2.7817(8), Ir3−Mo1 2.8043(8), Mo1−Mo4 2.8925(10), Ir5−Mo1 2.6988(8), Rh7−Mo1 2.7352(10), Ir2−Ir3 2.6965(5), Ir2−Mo4 2.8478(8), Ir2−Ir5 2.7322(7), Ir2−Mo6 2.8648(8), Ir2−Rh7 2.8281(8), Ir3−Mo4 2.7318(8), Ir3−Ir5 2.6837(6), Ir3−Mo6 2.8727(8), Rh7−Mo4 2.8351(9), Ir5−Mo6 2.7552(9), Mo1−C17 2.008(8), Ir2−C22 1.879(8), Ir2−C21 1.878(8), Ir3−C31 1.868(9), Ir3−C32 1.907(8), Ir3−C34 2.456(9), Mo4−C34 2.006(9), Mo4−C47 2.004(8), Ir5−C51 1.867(8), Ir5−C52 1.861(8), Ir5−C56 2.526(9), Mo6-C61 1.993(10), Mo6−C56 1.946(9), Rh7−C17 2.188(8), Rh7−C47 2.163(8).

There are three distinct groups of type C clusters. Gold-rich examples are not expected to conform to PSEPT rules. These 90 CVE species are comprised of an $Au_6(PPh_3)_6$ moiety and a 12-electron metal/ligands/charge combination. As expected, the group 8 metal-containing clusters with π-acceptor ligands $Ru_2Os_5(CO)_{15}(\eta^5\text{-}C_5H_5)_2$, $Os_7(\mu\text{-}S(CH_2)_2OCH_2CH_2)(CO)_{18}$, and $Os_7(CO)_{17}(\eta^6\text{-}C_6H_6)$ do observe the 96 CVE-predicted count. The two group 6/group 9 mixed-metal clusters $W_3Ir_4(\mu\text{-}H)(CO)_{12}(\eta^5\text{-}C_5H_5)_3$ (**3**) [17] (94 CVE) and $Mo_3RhIr_3(\mu\text{-}CO)_4(CO)_7(\eta^5\text{-}C_5H_5)_3(\eta^5\text{-}C_5Me_5)$ (**2**) (96 CVE) with this geometry are unusual in their lack of consistency in electron count, which prompted a more detailed study using DFT.

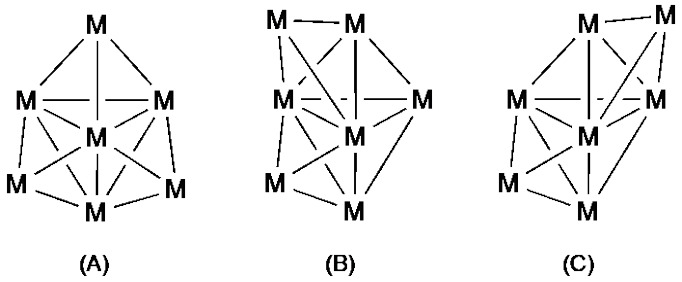

Type A

$Ru_3CoAu_3(CO)_{12}(PPh_3)_3$ 96 CVE [18]

$Ru_4Au_3(\mu_3\text{-}H)(CO)_{12}(PPh_3)_3$ 96 CVE [21]

$Ru_3Au_4(\mu_3\text{-}CMe)(Br)(CO)_9(PPh_3)_3$ 96 CVE [23]

$Os_6Au(\mu\text{-}H)(CO)_{16}(PEt_3)(SbPh_3)$ 96 CVE [25]

$RuOs_5Au(CO)_{15}(PPh_3)(\eta^5\text{-}C_5H_5)$ 96 CVE [27]

$Os_3Rh_4(\mu_3\text{-}\eta^6\text{-}C_6H_5CH_3)(CO)_{13}$ 92 CVE [15]

Type C

$[PtAu_6(CO)(PPh_3)_7]^{2+}$ 90 CVE [19, 20]

$[VAu_6(CO)_4(PPh_3)_6]^{+}$ 90 CVE [22]

$[CoAu_6(CO)_2(PPh_3)_6]^{+}$ 90 CVE [24]

$[PdAu_6(CNC_6H_3Me_2\text{-}2,6)_2(PPh_3)_6]^{2+}$ 90 CVE [26]

$Ru_2Os_5(CO)_{15}(\eta^5\text{-}C_5H_5)_2$ 96 CVE [28]

$Os_7(\mu\text{-}S(CH_2)_2OCH_2CH_2)(CO)_{18}$ 96 CVE [29]

$Os_7(CO)_{17}(\eta^6\text{-}C_6H_6)$ 96 CVE [30]

$W_3Ir_4(\mu\text{-}H)(CO)_{12}(\eta^5\text{-}C_5H_5)_3$ (**3**) 94 CVE [17]

$Mo_3RhIr_3(CO)_{11}(\eta^5\text{-}C_5H_5)_3(\eta^5\text{-}C_5Me_5)$ (**2**) 96 CVE

Figure 3. Bicapped trigonal bipyramidal core isomers and structurally verified heptametallic clusters.

2.3. Theoretical studies

The formally electron deficient cluster $W_3Ir_4(\mu\text{-}H)(CO)_{12}(\eta^5\text{-}C_5H_5)_3$ (**3**) is related to **2** by conceptual replacement of one of the iridium atoms with a rhodium atom, replacement of the tungsten atoms with molybdenum atoms, and addition of a CO ligand. Theoretical studies of **2** and **3** to rationalize their stability with varying electron counts have therefore been carried out. Removal of two electrons from **2** is readily accomplished by removal of a CO ligand. While there are many possible ligand removals, we have chosen to remove a ligand from the metal with the most intermetallic bonding and highest formal electron count (Ir2 has 19 electrons and six distinct Ir2-M bonds). One CO ligand was therefore removed from Ir2 in **2** to afford the (theoretical) 2-electron deficient species [**2**−CO]. The geometry-optimized structure of [**2**−CO] is shown in Figure S1, with important bond lengths collected in Table S2. The location of a CO ligand face-capping the Ir1/Mo4/Rh7 face helps alleviate the formal electron-deficiency of Ir2. Gibbs free energies for the theoretical CO dissociation reaction **2** → [**2**−CO] + CO are 20.0 kcal mol^{-1} and 23.7 kcal mol^{-1} by methods BP and PBE,

respectively (Table S3 and S4), consistent with the observed stability of **2**. In the same manner, one CO ligand was added to W3 in **3** to obtain an electron-precise species [**3**+CO], because W3 formally has the least electrons of all the metal atoms. The geometry optimized [**3**+CO] has a face-capping CO located at the W3/Ir3/Ir4 face (Figure S3). The calculated lengths of the W3-M bonds increase proceeding from **3** to [**3**+CO]. In particular, W1−W3 [2.937 Å (BP) and 2.930 Å (PBE)] is significantly increased in [**3**+CO], compared to the value for **3** (2.784(2) Å) which was suggested as sufficiently short to perhaps be a W=W double bond[17] at the time of the X-ray structural study (Table S2). The Gibbs free energies of the proposed dissociation reaction [**3**+CO] → **3** + CO are −9.5 kcal mol^{-1} and −5.4 kcal mol^{-1} by methods BP and PBE, respectively (Table S3 and S4), consistent with the observed stability of **3**. We emphasize that the location choices of CO removal/addition are somewhat arbitrary, but within the range of possible options, the locations chosen are plausible and likely to afford similar or indeed lower energy species than other options.

We have also examined the linear optical absorption spectrum of cluster **2** (Figure S5), which exhibits four distinct maxima [ν = 11150 cm^{-1}, ε = 1031 cm^{-1} M^{-1}; ν = 17750 cm^{-1}, ε = 4081 cm^{-1} M^{-1}; ν = 24400 cm^{-1}, ε = 9347 cm^{-1} M^{-1}; ν = 28500 cm^{-1}, ε = 14788 cm^{-1} M^{-1}]. To assign the observed bands in cluster **2**, a time-dependent DFT (TDDFT) study was performed which nicely reproduced the experimental spectrum, as shown in Figure S5. The major visible transition at 17750 cm^{-1} (calculated at 17422 cm^{-1}) is mainly attributed to transition from the HOMO-2 (38%) to the LUMO+3 orbitals, with significant charge displacement across the cluster core. The observed absorption at 24400 cm^{-1}, calculated at 24997 cm^{-1}, is attributed to the HOMO-1 (48%) to LUMO+7 transition, with significant charge displacement from molybdenum to the CO ligands. The relevant molecular orbitals are shown in Figure S6.

2.4. Conclusion

The present studies have afforded $Mo_3Ir_3(\mu_4\text{-}\eta^2\text{-}CO)(\mu_3\text{-}CO)(CO)_{10}(\eta^5\text{-}C_5H_5)_3$ (**1**) in poor yield (16%), but in an improved yield compared to that of its (methylcyclopentadienyl)tungsten analogue (6%).[13] This has provided the initial opportunity to explore the reactivity of these group 6-group 9 edge-bridged trigonal bipyramidal clusters. In the present work, reaction with $Rh(CO)_2(\eta^5\text{-}C_5Me_5)$ has demonstrated the efficacy of this putative rhodium-containing capping agent; while the

reaction has been shown to lack specificity, it has afforded the largest molybdenum-rhodium-iridium cluster thus far, namely $Mo_3RhIr_3(\mu\text{-}CO)_4(CO)_7(\eta^5\text{-}C_5H_5)_3(\eta^5\text{-}C_5Me_5)$ (**2**), in only the second report of a cluster with this metal combination.[13]

The spectroscopic and structural studies have confirmed the compositions of **1** and **2**, and revealed that **2** possesses 96 CVE, in contrast to the only extant cluster with this core geometry, and possessing metals from the same groups in the Periodic Table $[W_3Ir_4(\mu\text{-}H)(CO)_{12}(\eta^5\text{-}C_5H_5)_3]$ (**3**), 94 CVE]. Free-energy calculations are consistent with the greater stability of the experimentally isolated **2** and **3**, rather than the possible [**2**-CO**]** or [**3**+CO**]** alternatives.

We have previously noted the proclivity to cap tetrahedra on core nuclearity increase in the group 6-group 9 mixed-metal cluster system, with a tetracapped tetrahedral cluster the most extreme example,[10] rather than the more conventional core expansion via capping of octahedral cores seen with many transition metal clusters bearing π-acceptor ligands. The structure of **3** provides a further example of cluster build-up by the fusing of tetrahedra with this combination of transition metal atoms.

3. Experimental

Reactions were performed under an atmosphere of nitrogen using standard Schlenk techniques, although no precautions were taken to exclude air in the work-ups. Solvents were AR grade and distilled under nitrogen using standard methods: CH_2Cl_2 over CaH_2 and toluene over sodium benzophenone ketyl radical. All other solvents and reagents were obtained commercially and were used as received. Petrol refers to a fraction of boiling range 60–80 °C. Cluster products were purified by preparative thin-layer chromatography (TLC) on 20 × 20 cm glass plates coated with Merck GF_{254} silica gel (0.5 mm). Analytical TLC was conducted on aluminum sheets coated with 0.25 mm Merck GF_{254} silica gel. Literature procedures were used to synthesize $Mo_2Ir_2(\mu\text{-}CO)_3(CO)_{10}(\eta^5\text{-}C_5H_5)_2$ [31] and $Rh(CO)_2(\eta^5\text{-}C_5Me_5)$ [32].

Infrared spectra were recorded on PerkinElmer System 2000 and PerkinElmer Spectrum One FT-IR spectrometers using a CaF_2 solution cell and AR grade CH_2Cl_2 solvent; spectral

features are reported in cm^{-1}. ^1H NMR spectra were recorded on a Bruker Ascend-400 spectrometer at 400 MHz in $CDCl_3$ (Cambridge Isotope Laboratories) and referenced to non-deuterated solvent (δ 7.26). ESI mass spectra were recorded on a Micromass-Waters LC-ZMD single quadrupole liquid chromatograph-MS instrument, and are reported in the form: *m*/*z* (assignment, relative intensity). Microanalyses were carried out at the School of Human Sciences, Science Centre, London Metropolitan University, UK.

*3.1. Synthesis of $Mo_3Ir_3(\mu_4\text{-}\eta^2\text{-}CO)(\mu_3\text{-}CO)(CO)_{10}(\eta^5\text{-}C_5H_5)_3$ (**1**).*

A solution of $Mo_2Ir_2(\mu\text{-}CO)_3(CO)_7(\eta^5\text{-}C_5H_5)_2$ (30.0 mg, 30.2 μmol) in toluene (20 mL) was refluxed for 30 min, the extent of reaction being monitored by IR spectroscopy. The solution was taken to dryness in vacuo, and the crude residue dissolved in a minimum amount of CH_2Cl_2. Purification on silica preparative TLC plates, eluting with CH_2Cl_2/petrol (5:1), afforded five bands. The contents of the first band (R_f = 0.8, orange) were extracted with CH_2Cl_2 and reduced in volume to afford an orange solid identified as unreacted $Mo_2Ir_2(\mu\text{-}CO)_3(CO)_7(\eta^5\text{-}C_5H_5)_2$ (8.9 mg, 9.0 μmol, 30%). The contents of the second band (R_f = 0.6, brown) and the third band (R_f = 0.4, brown) were extracted with CH_2Cl_2 and reduced in volume to afford thus-far unidentified brown solids. The contents of the fourth band (R_f = 0.3, brown) were extracted with CH_2Cl_2 and reduced in volume to afford a brown solid identified as $Mo_3Ir_3(\mu_4\text{-}\eta^2\text{-}CO)(\mu_3\text{-}CO)(CO)_7(\eta^5\text{-}C_5H_5)_3$ (**1**, 4.5 mg, 3.2 μmol, 16%). The contents of the fifth band (R_f = 0.1, brown) were in trace amounts and were not isolated.

Characterization data for **1**: IR (CH_2Cl_2): ν(CO) 2067 w, 2042 vs, 2012 vs, 1998 s, 1989 w, 1969 w, 1947 w, 1929 m, ν(μ-CO) 1878 m, 1698 w cm^{-1}. ^1H NMR ($CDCl_3$): δ 5.72 (s, 5H, C_5H_5), 5.44 (s, 5H, C_5H_5), 5.34 (s, 5H, C_5H_5). HR-MS (ESI): calculated for $C_{27}H_{15}Ir_3Mo_3O_{12}$, 1397.6544 ($[M]^+$); found, 1397.6576 ($[M]^+$, 1). Analysis: calculated for $C_{27}H_{15}Ir_3Mo_3O_{12}$: C 23.23, H 1.08; Found C 23.22, H 1.07.

*3.2. Synthesis of $Mo_3RhIr_3(\mu\text{-}CO)_4(CO)_7(\eta^5\text{-}C_5H_5)_3(\eta^5\text{-}C_5Me_5)$ (**2**)*

$Rh(CO)_2(\eta^5\text{-}C_5Me_5)$ (3.9 mg, 13.3 μmol) was added to a brown solution of $Mo_3Ir_3(\mu_4\text{-}\eta^2\text{-}CO)(\mu_3\text{-}CO)(CO)_{10}(\eta^5\text{-}C_5H_5)_3$ (**1**, 9.8 mg, 7.0 μmol) in CH_2Cl_2 (30 mL), and the solution was heated at reflux for 24 h, the extent of reaction being monitored by IR spectroscopy. The

solution was taken to dryness in vacuo, and the crude residue was dissolved in a minimum amount of CH_2Cl_2 and applied to a silica preparative TLC plate. Elution with CH_2Cl_2 afforded two bands. The contents of the first band (R_f = 0.8, brown) were extracted with CH_2Cl_2 to afford a brown solid identified as unreacted starting cluster **1** (4.2 mg, 3.0 μmol, 43%). The contents of the second band (R_f = 0.5, brown) were extracted with CH_2Cl_2 to afford a brown solid identified as $Mo_3RhIr_3(\mu\text{-}CO)_4(CO)_7(\eta^5\text{-}C_5H_5)_3(\eta^5\text{-}C_5Me_5)$ (**2**, 4.8 mg, 3.0 μmol, 42 %).

Characterization data for **2**: IR (CH_2Cl_2): ν(CO) 2023 vs, 1994 vs, 1941 m, ν(μ-CO) 1797 br, 1711 br cm^{-1}. ^1H NMR ($CDCl_3$): δ 5.33 (s, 5H, C_5H_5), 5.28 (s, 5H, C_5H_5), 4.82 (s, 5H, C_5H_5), 2.10 (s, 15H, C_5Me_5). HR-MS (ESI): calculated, $C_{36}H_{30}Ir_3Mo_3O_{11}Rh$, 1613.6894 ($[M]^+$); found, 1613.7047 ($[M]^+$, 18). The cluster slowly decomposed over a period of days, precluding satisfactory elemental analysis.

3.3 Computational studies

Computational studies were carried out using the Amsterdam Density Functional (ADF) program, version 2013 [33]. Calculations were executed on the raijin supercomputer housed at the ANU Supercomputer Facility and operated under the National Computer Infrastructure Scheme. The calculations employed all-electron basis sets of triple-ζ quality with a single polarization function (TZP), spin-unrestricted on each atom. Relativistic effects were accounted for using the zero-order relativistic approximation (ZORA) [34]. Geometry-optimized calculations were carried out with gradient-corrected exchange–correlation functionals (generalized gradient approximation: GGA), suggested by BP [35] or PBE [36] in a self-consistent fashion. BP or PBE optimizations were repeated with the inclusion of solvent effects through the conductor-like screening model (COSMO) method using parameters appropriate to solvation by dichloromethane [38]. Gibbs free energy data were obtained through frequency calculations [38].

Acknowledgements

We thank the Australian Research Council (ARC) for support of this work. J.F. was the recipient of a China Scholarship Council ANU Postgraduate Scholarship and M.D.R. was the recipient of an Australian Postgraduate Award.

Supplementary material

Crystallographic data for **1** and **2**, X-ray and geometry-optimized structures of **2** and **3**, experimental and computational linear optical absorption data for **2**, and complete computational data are included in the **Supplementary material**. CCDC 1047904 (**1**) and 1501036 (**2**) contain the supplementary crystallographic data for this paper. These data can be obtained free of charge from The Cambridge Crystallographic Data Centre via www.ccdc.cam.ac.uk/structures.

References

[1] R.D. Adams, F.A. Cotton, Catalysis by Di- and Polynuclear Metal Cluster Complexes, Wiley-VCH, New York, 1998.

[2] P. Buchwalter, J. Rosé, P. Braunstein, Chem. Rev. 115 (2015) 28-126.

[3] C. Zhang, Y. Song, X. Wang, Coord. Chem. Rev. 251 (2007) 111-114.

[4] D.W. Goodman, J.E. Houston, Science 236 (1987) 403-409.

[5] M. Ichikawa, Adv. Catal. 38 (1992) 283-400.

[6] C. Zhang, Y. Cao, J. Zhang, S. Meng, T. Matsumoto, Y. Song, J. Ma, Z. Chen, K. Tatsumi, M.G. Humphrey, Adv. Mater. 20 (2008) 1870-1875.

[7] M.C. Comstock, J.R. Shapley, Coord. Chem. Rev. 143 (1995) 501-533.

[8] N.T. Lucas, J.P. Blitz, S. Petrie, R. Stranger, M.G. Humphrey, G.A. Heath, V. Otieno-Alego, J. Am. Chem. Soc 124 (2002) 5139-5153.

[9] M.D. Randles, P.V. Simpson, V. Gupta, J. Fu, G.J. Moxey, T. Schwich, A.L. Criddle, S. Petrie, J.G. MacLellan, S.R. Batten, R. Stranger, M.P. Cifuentes, M.G. Humphrey, Inorg. Chem. 52 (2013) 11256-11268.

[10] J. Fu, G.J. Moxey, M.P. Cifuentes, M.G. Humphrey, J. Organomet. Chem. 792 (2015) 46-50.

[11] M.D. Curtis, W.M. Butler, J. Organomet. Chem. 155 (1978) 131-145.

[12] M.D. Randles, P.V. Simpson, V. Gupta, J. Fu, G.J. Moxey, T. Schwich, A.L. Criddle, S. Petrie, J.G. MacLellan, S.R. Batten, R. Stranger, M.P. Cifuentes, M.G. Humphrey, Inorg. Chem. 52 (2013) 11256-11268.

[13] E.G.A. Notaras, N.T. Lucas, M.G. Humphrey, J. Organomet. Chem. 631 (2001) 139-142.

[14] D.M.P. Mingos, Acc. Chem. Res. 17 (1984) 311-319.

[15] J.P.-K. Lau, Z.-Y. Lin, W.-T. Wong, Angew. Chem. Int. Ed. 42 (2003) 1935-1937.

[16] M. Kulzick, R.T. Price, E.L. Muetterties, V.W. Day, Organometallics 1 (1982) 1256-1258.

[17] S.M. Waterman, M.G. Humphrey, D.C.R. Hockless, Organometallics 15 (1996) 1745-1748.

[18] M.I. Bruce, B.K. Nicholson, Chem. Commun. (1982) 1141-1143.

[19] L.N. Ito, J.D. Sweet, A.M. Mueting, L.H. Pignolet, M.F.J. Schoondergang, J.J. Steggerda, Inorg. Chem. 28 (1989) 3696-3701.

[20] D.A. Krogstad, V.G. Young Jr., L.H. Pignolet, Inorg. Chim. Acta 264 (1997) 11-32.

[21] M.I. Bruce, B.K. Nicholson, J. Organomet. Chem. 252 (1983) 243-255.

[22] K. Wurst, J. Strähle, G. Beuter, D.B. Dell'Amico, F. Calderazzo, Acta Chem. Scand. 45 (1991) 844-849.

[23] M.I. Bruce, P.A. Humphrey, B.W. Skelton, A.H. White, J. Organomet. Chem. 689 (2004) 2558-2561.

[24] M. Holzer, J. Strahle, G. Baum, D. Fenske, Z. Anorg. Allg. Chem. 620 (1994) 192-198.

[25] P.G. Stones, P.R. Raithby, in Cambridge Crystallographic Database, CSD refcode IDEPOX, 2006.

[26] N.H. Takata, A.M.P. Felicıssimo, V.G. Young Jr., Inorg. Chim. Acta 325 (2001) 79-84.

[27] M.R.A. Al-Mandhary, R. Buntem, C.L. Doherty, A.J. Edwards, J.F. Gallagher, J. Lewis, C.-K. Li, P.R. Raithby, M.C.R. de Arellano, G.P. Shields, J. Cluster Sci. (2005) 16127-16150.

[28] J. Lewis, C.A. Morewood, P.R. Raithby, M.C.R. de Arellano, Dalton Trans. (1996) 4509-4510.

[29] K.S.-Y. Leung, W.-T. Wong, Eur. J. Inorg. Chem. (1999) 1757-1763.

[30] J. Lewis, C.-K. Li, C.A. Morewood, M.C.R. de Arellano, P.R. Raithby, W.-T. Wong, Dalton Trans. (1994) 2159-2165.

[31] N.T. Lucas, M.G. Humphrey, D.C.R. Hockless, J. Organomet. Chem. 535 (1997) 175-181.

[32] N. Dunwoody, S.-S. Sun, A.J. Lees, Inorg. Chem. 39 (2000) 4442-4451.

[33] ADF2013, SCM Theoretical Chemistry, Vrije Universiteit: Amsterdam, The Netherlands. http://www.scm.com.

[34] E. van Lenthe, A. E. Ehlers, E. J. Baerends, J. Chem. Phys. 110 (1999) 8943-8953.

[35] a) A. D. Becke, Phys. Rev. A 38 (1998) 3098-3100; b) J. P. Perdew, Phys. Rev. B 33 (1986) 8822-8824.

[36] J. P. Perdew, K. Burke, M. Ernzerhof, Phys. Rev. Lett. 77 (1996) 3865-3868; b) J. P. Perdew, K. Burke, M. Ernzerhof, Phys. Rev. Lett. 78 (1997) 1396.

[37] a) A. Klamt, G. Schuurmann, J. Chem. Soc., Perkin Trans. 2 1993, 799-805; b) J. Andzelm, C. Kolmel, A. Klamt, J. Chem. Phys. 103 (1995) 9312-9320.

[38] a) M. Swart, E. Rösler, , F. M. Bickelhaupt, J. Comp. Chem. 27 (2006) 1486-1493; b) M. Swart, F. M. Bickelhaupt, J. Chem. Theory Comp. 2 (2006) 281-287.